EVS36 Symposium
Sacramento CA, USA, June 11-14, 2023

Droop Rate Controlled DC Bus Charging Plaza

Edward Heath[1], Jos Warmerdam[1], Rob Schaacke[1]

[1]*Amsterdam University of Applied Sciences, Faculty of Technology, City Net Zero, Energy & Innovation group*
e.p.heath@hva.nl

Executive Summary

A lab-based test setup was developed to simulate a novel droop rate controlled DC bus charging plaza installation in the Netherlands. The system consists of multiple bidirectional DC charging points, a PV array and a bidirectional grid connection. Currently the installed system employs linear droop control at the charge points and active grid connection. This lab setup allows for the testing of new control schemes, such as piecewise linear droop control, before implementing in the installed system. The simulations performed in this study investigate a variety of power flow scenarios and determine appropriate voltage and current setpoints and control mechanisms.

1 Introduction

As DC power sources and loads become more prevalent, so too does the motivation to develop DC power grids. In this project an AC grid-connected DC network has been formed to facilitate low speed EV charging with the addition of a PV array. Conventional EV charging plazas operate on an AC bus and require separate communication lines to monitor an assortment of parameters, that must conform to certain standards and communication protocols, all controlled by a central energy management system (EMS). This communication network is liable to fault, interference, or message delays, all of which could result in disruption to the system to a varying extent and in the worst case system failure.

Due to this increasing interest in the applicability of DC networks many studies have been performed to determine the best method of system control. Consensus being that voltage droop control is the best suited decentralised primary control method, although there is some payoff between current sharing and bus voltage deviation [1, 2, 3]. The focus of study has thus been concerned with accurate load current sharing amongst sources and the reliable regulation of bus voltage. The difficulty in accurate load current sharing is that each converter, connected in parallel to a common bus, measures a different voltage due to the inherent voltage drop caused by line impedance. This line impedence has a detrimental effect on the load current sharing for systems employing fixed linear droop characteristics.

To solve this issue, [4] propose the integration of a power flow controller to better regulate power amongst sources whilst the network voltage is regulated by the grid connecting converter. They showed that during times when the grid connecting controller was not able to reliably regulate the network voltage, the power based droop controller could transition from a power sharing mode to a bus regulation mode to stabilise the voltage. Low bandwidth power line communication (LBC) was utilised to exchange current and voltage information between the decentralised droop controllers in [1]. This improved current sharing accuracy and the system voltage was better regulated. [2] also used LBC and introduced a voltage shifting element that corrected for the voltage drop experienced by each source controller. A robust adaptive droop control was implemented in [5] which does not require in-depth knowledge of the system in question. Simply put, this method changes the characteristics of the droop curve to the desired position, considering the network criteria. In a move towards standardisation [3] develops a hierarchical control framework in which droop control comprises the primary control and ensures the parallel operation of the controllers. Secondary control is

implemented to regulate the voltage back to the network nominal value. The tertiary control dictates how the DC network interacts with the AC grid.

The properties of this system are different to that of conventional droop control theory, in that the system can operate reliably within a wide voltage range depending on the source and load profile present. Thus, it is not necessary to directly regulate the voltage to a nominal value. An energy management system (EMS) can alter V-I response of each controller for a variety of scenarios, such as prioritising charging/discharging of EVs or a static battery, or delivering power to or drawing power from the AC grid. This study aims to incorporate the piecewise linear droop curve, presented in [6], to control a variety of sources and loads in a decentralized and autonomous way within a wide voltage range. It is of note that this project is ongoing and as such the progress so far is presented.

1.1 The Installation

This project, in partnership with A.S.R., Kropman, Venema, and DC Systems, has installed 3 bidirectional 10 kW DC chargers on a single 700 V DC bus with an active front end (AFE) bi-directional connection to the AC power grid, as depicted in Fig 1. The AFE is a galvanically isolated connection to the AC grid and active voltage source [7] developed by DC Systems. A 40 kWp PV array is connected to the DC bus via a controller which determines if the PV power should flow to an on-site battery, the EV chargers, or to the AC-grid. It is an active DC installation whereby the voltage level, power flow, and fault level are all managed locally and autonomously, with multiple active elements such as the active front end (AFE), bi-directional chargers, and PV array. Additionally, the system has a safety wire, marked in a green dashed line in Fig 1, and slow speed communication line. Due to the prescence of multiple distributed sources there is a chance one source may not have been shut down before maintenance. The safety wire delivers a signal to all converters in the system, separate to the main power cables, that indicate if the converters should be active or not.

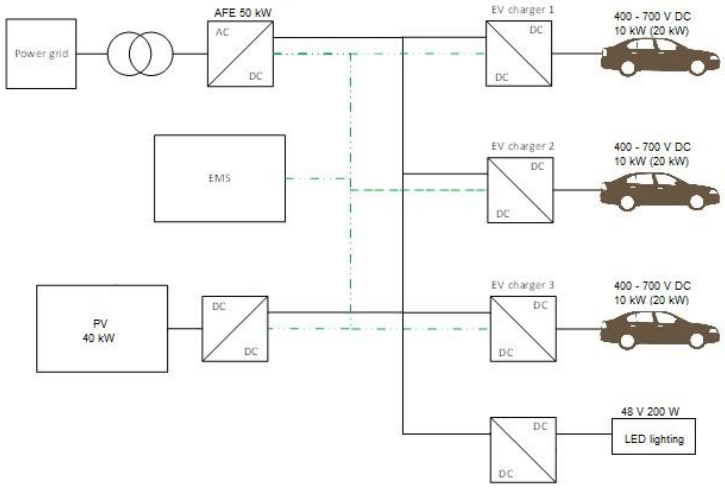

Figure 1: VAP-DC installed system architecture. The safety wire is represented by the dashed green line

1.2 The Lab Simulation System

The equipment being used to run the lab simulations are the Delta-Elektronika SM15K-series controllable DC power supplies (CPS) [8], namely 4 x SM500-CP-90 and 1 x SM1500-CP-30. The configuration is presented in Fig 2. The SM500s can be connected in parallel using a master/slave configuration to boost their total maximum voltage to 1000 V. In this way it is possible to simulate 3 devices that operate at the nominal 700 V DC bus voltage, as in the case of the installed system. Alternatively, the system voltage could be scaled to allow for the use of more than 3 devices. Current lab simulation practise is to use 3 devices at a nominal 350 V, a standard DC network voltage. The SM1500-CP-30, which can operate up to 1500 V, is connected to the installed system in Utrecht as a point of entry to validate the model used in the lab simulations and make further system measurements. Here the Python code was tested by controlling the CPS in a variety of scenarios.

Figure 2: Lab simulation setup showing the 4 Delta Elektronika CPSs and a laptop to run the simulations, connected by ethernet link

2 Droop Control

In DC power systems, droop control is an autonomous method of controlling power output from source controllers in response to system voltage variations caused by an over- or under-supply of power in a network [1, 2, 4, 6, 9]. In this sense it is analogous to the frequency response of an AC power system, and is therefore a primary control method. With the VAP-DC system topology in mind, an over voltage will occur when the PV array delivers an abundance of power relative to the power demand of the EV chargers. A voltage below the nominal will occur when an extra EV load is connected resulting in a large power demand.

The benefits of such a control system are the relative ease of and reduced cost of implementation with respect to a generic communication line and central EMS system, the increased speed of system response due to the lack of communication signal delivery and processing, and the added security in cases of communication line failure or hacking. In conventional DRC, the output voltage of a power source is calculated with equation 1.

$$V_o = v_{ref} - r_d \cdot i_o \tag{1}$$

Where v_{ref} is the voltage under no load, r_d is the droop coefficient, and i_o is the controller output current. r_d is effectively the gradient dI/dV for a given controller.

2.1 Implementation

In this lab based system, each device connected to the network is directly and autonomously controlled by a predetermined V-I response curve, such that for every measured voltage an output current is set. The bus voltage is allowed to vary between values of 320 V - 380 V, analogous to 640 V – 760 V in the installed system. Thus, voltage does not need to be regulated back to a fixed nominal value.

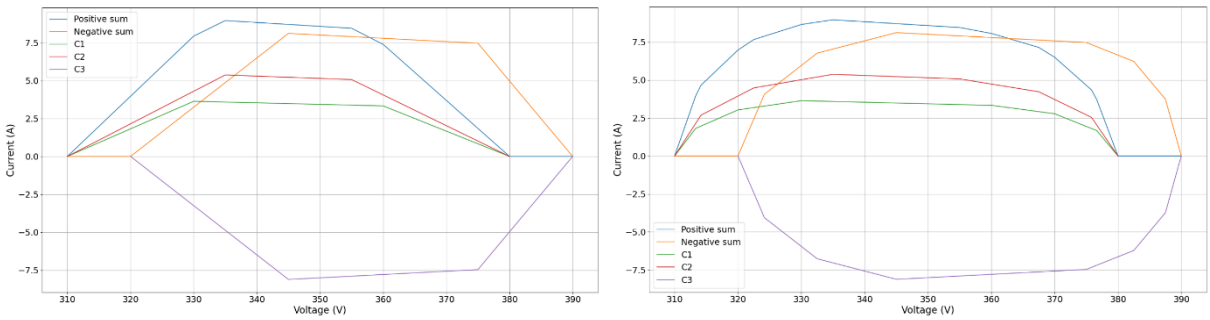

Figure 3: Droop curves for three devices, sources C1 and C2, and load C3. The sum of the sources is plotted in blue, the inversed sum of the loads is plotted in yellow. Left) Linear droop curves. Right) Piecewise linear droop curves.

Piecewise linear droop control (PWLD) provides improved load sharing in a distributed and meshed DC network in response to cable impedances by splitting the linear droop into a series of linear droops, as developed and described in [6]. If a load is connected to the network, the network voltage will drop. A larger load leads to a larger voltage drop. So if source A has a linear droop with a steep gradient, the change in current provided will be greater than source B with a shallow gradient linear droop. A higher gradient droop has a larger dI/dV. The piecewise linear droop curve is formulated such that it has a low droop value for a small load, and a high droop value for a large load. In other words, the gradient gets steeper the further from nominal voltage the system is.

The lab setup consisted of a combination of load, source, and bidirectional devices. The naming convention of the controllers are CX. The number is of no importance and merely an identification tag. The CPSs used in this setup are self regulating operating in voltage controlled or current controlled modes. To not suffer the voltage controlled mode a voltage operating window has been accounted for (as with the installed system) and the output currents are altered in response to the measured bus voltage. The bus voltage is in turn determined by the intersection of the sum of source and inversed sum of load currents, as in Fig 3. In this manner not only are sources droop controlled, so too are the loads. Loads and sources that are not outputting the highest current all experience some degree of voltage drop with respect to the highest power source.

A V-I curve is formed for each device in the system, as shown in Fig 3. At each time step the network voltage and current of each device is measured. The measured voltage is then compared to the V-I curve of the respective devices and the corresponding current is determined. This current is the ideal value at the measured voltage. The ideal current, I_{Target}, corresponding to the measured bus voltage, is then compared against the conditionals regarding maximum allowed current step size, I_{Step}, as presented in equation 2, and the maximum and minimum allowable device output current. I_{Step} will be positive or negative depending on whether I_{Target} is larger or less than than I_{Meas}.

$$I_{Setpoint}\begin{cases} I_{Target}, & \left|I_{Target}-I_{Meas}\right| \le I_{Step} \\ I_{Meas}+I_{Step}, & \left|I_{Target}-I_{Meas}\right| > \left|I_{Step}\right| \end{cases} \tag{2}$$

A proportional-integral (PI) control algorithm was implemented to the output current, equation 3, such that the error between the measured current and the setpoint current, equation 4, stimulates an appropriate response. It is worth noting that a maximum dI/dt was defined at 20 A/s. Conventional PI control depends on a feedback loop, whereby the process variable is iteratively corrected towards the setpoint value. Due to processing speed limitations and the desired time step of the system this PI control has one control step per time step. The integral term then increases/decreases with the error over time. A large voltage drop, due to the connection of an EV load will result in a large instantaneous error between a source output current and the new ideal value for the given bus voltage. This will result in the integral term increasing with time until the error has decreased sufficiently and the system is operating at a stable bus voltage.

$$I_{New} = I_{Meas} + K_P \cdot e(t) + K_I \cdot \int_0^t e(t)\,dt \tag{3}$$

$$e(t) = I_{Setpoint,t} - I_{Meas,t} \tag{4}$$

Tuning of K_P, K_I, time step, and maximum current step allow for a more stable network voltage due to faster responding and better controlled devices.

In Fig 3 the V-I curves are created using the linear droop and the described PWLD method. Fig 4 extends this to an s-shaped PWLD curve. C1 is also formed as a bidirectional device, suich that at time of undersupply it acts as a source, and times of oversupply it acts as a load. The hypothesis was that the s-shaped PWLD curve would slow dI/dV when using a bi-directional device, with respect to a regular PWLD curve.

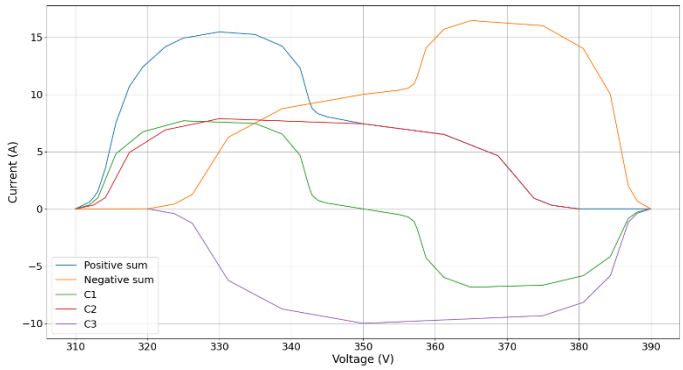

Figure 4: Droop curves for three controllers in an under-supplied system; source C2, load C3, and bidirectional C1. Plotted in yellow is the inverse of the load to clearly depict the stable voltage.

3 Experimental Results

This section presents the most recent results of this ongoing project. It is important to bear in mind that when making changes to the output power of a device during the test runtime, it is the maximum output power that is redefined. This is not necessarily the power that the device will then output, but rather the maximum power as defined in the V-I curve. The actual power is determined by the system voltage level as a result of overall power supply in the network, as previously discussed. Due to processing power limitations, the maximum sample rate per device was approximately 50 ms. Of course a fast sample rate is desirable since it would allow for a faster response time and therefore more stable system. The values $K_P = 0.1$ and $K_I = 0.1$ were used. This was found to be a good compromise between steady-state stability, i.e. the stability of current and therefore network voltage once ouput currents are approximately constant, and the dynamic response to power flow changes, however, it is possible these could be further tuned for improved performance.

3.1 General Power Changes

The maximum output powers were varied in a system with 3 devices, C1 as a bidirectional device, C2 as a pure source, and C3 as a pure load. The polarity of C1 switched from source to load and vice versa. Fig 5 shows the initial switching of steady state. At 22 s the maximum output power of C2 and C3 were switched in magnitude, such that C2 increased maximum output power to 2800 W whilst C3 reduced maximum output power to -1800 W. This moved the system from undersupplied to oversupplied, thus raising the network voltage. During this change, the bidirectional device, C1, switched from being a source to a load. This transition is not quite smooth due to the current not being correctly balanced between the devices at this time. There is a slight voltage overshoot as a result of the integrator term in the PI controller of output current. Fig 7 shows the network voltage deviation and the output current of C1 at the moment C1 switches output power polarity, in which the current of C1 bounces back to 0A. At 38 s the maximum output power of C1 was increased from 1200 W to 2500 W. This increased the dI/dV at the stable voltage for C1. This effect can be observed in Fig 6 at 38 s, where all currents then become more unstable, and as a result so too does network voltage. At 57 s the maximum output power of both C2 and C3 were again altered, such that C2 decreased to 2600 W and C3 increased to -3500 W. This resulted in an undersupplied network and caused C1 to revert to acting as a source. Finally at 77 s the maximum output power of C2 was further reduced to 1500 W. This didn't have a large effect on the network voltage because the decrease in power supplied by C2 was mostly covered by C1.

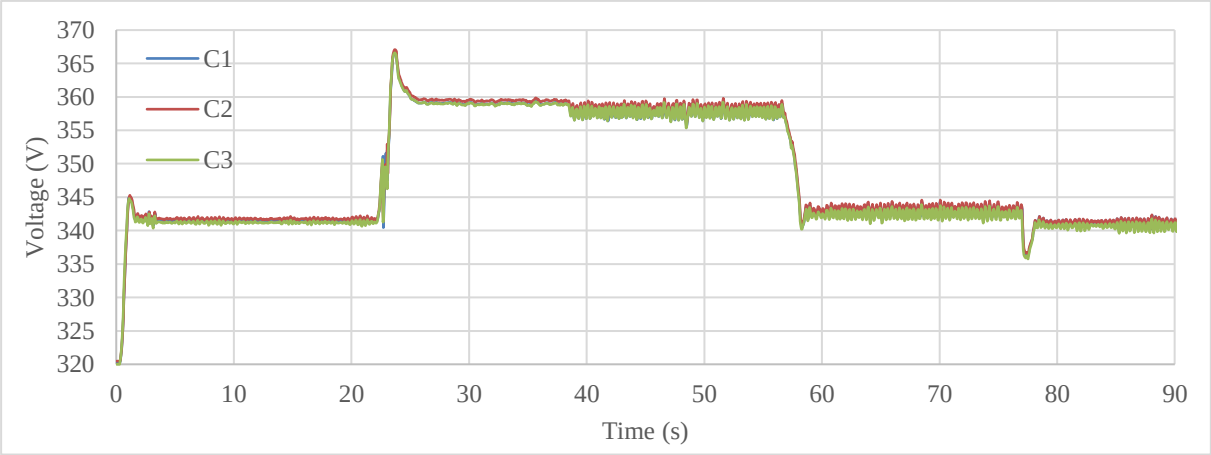

Figure 5: Variation in network voltage due to variations in device output powers

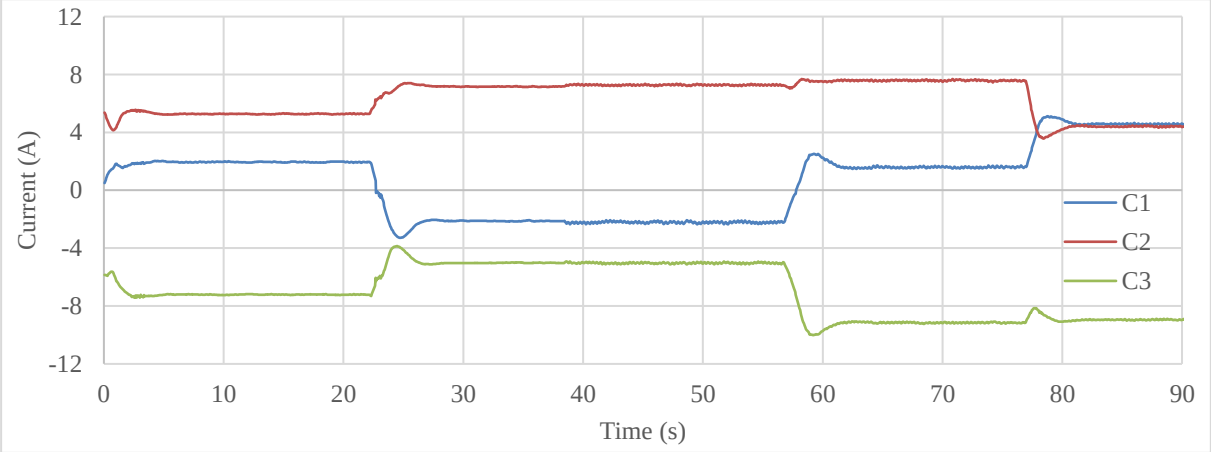

Figure 6: Variation in device output current

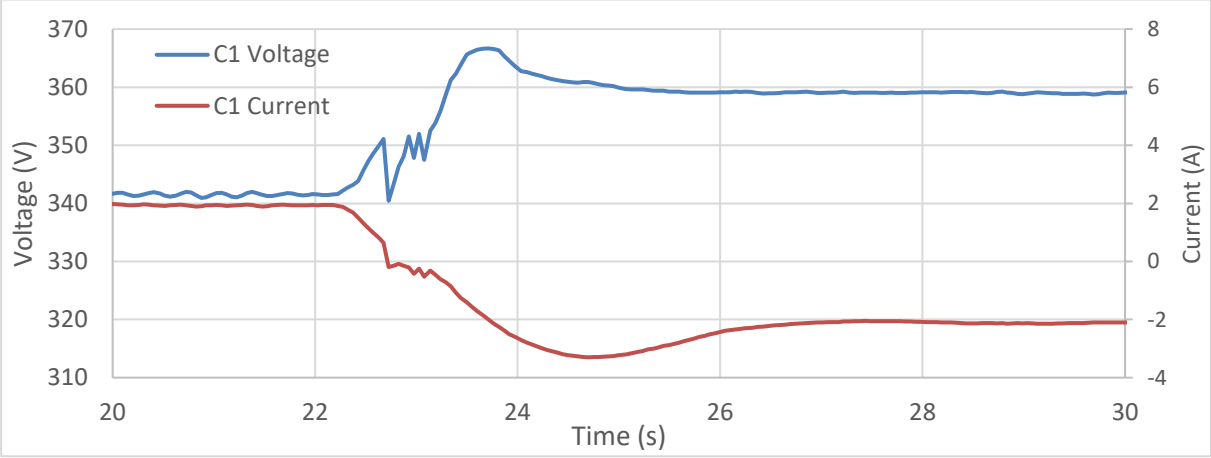

Figure 7: Output current and measured network voltage of C1 during polarity switching event

At 172 s the maximum output power of both C2 and C3 were changed to 2500 W and -2500 W, respectively, resulting in the V-I curves presented on the left in Fig 10 and causing the instability displayed in Fig 8. The stable voltage was then at the nominal 350 V which clearly caused all devices to react eratically as C1 switched rapidly between source and load. Fig 9 shows the output current of C3 spiked up to 16 A from -7 A, whilst the network voltage simultaneously spiked up to the maximum allowable network voltage of 380

V. It is thought that a parallel capacitor would improve system stability at these times, although, depending on the capacitance, it could introduce some additional safety considerations. However, the solution would require careful formation of the V-I curves including an improved power deadband for the bidirectional controller around nominal voltage. At 192 s the maximum output power of C2 was marginally decreased to 2400 W with little effect. At 210 s the maximum output powers of C2 and C3 were changed to 2200 W and -2600 W, respectively. This shifted the V-I curves to that which can be seen on the right in Fig 10.

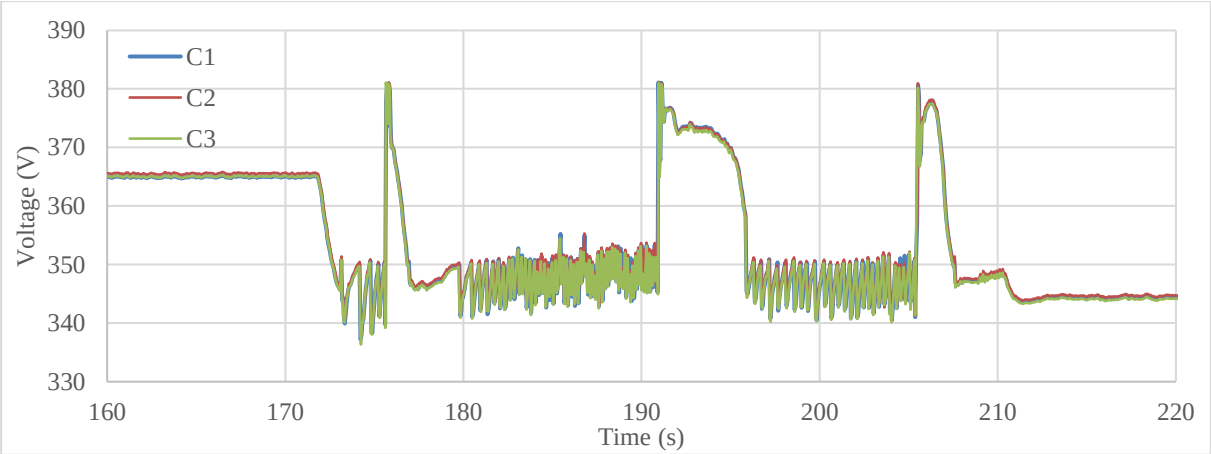

Figure 8: The network voltage when the stable voltage is at the nominal 350 V, where the bidirectional controller changes polarity.

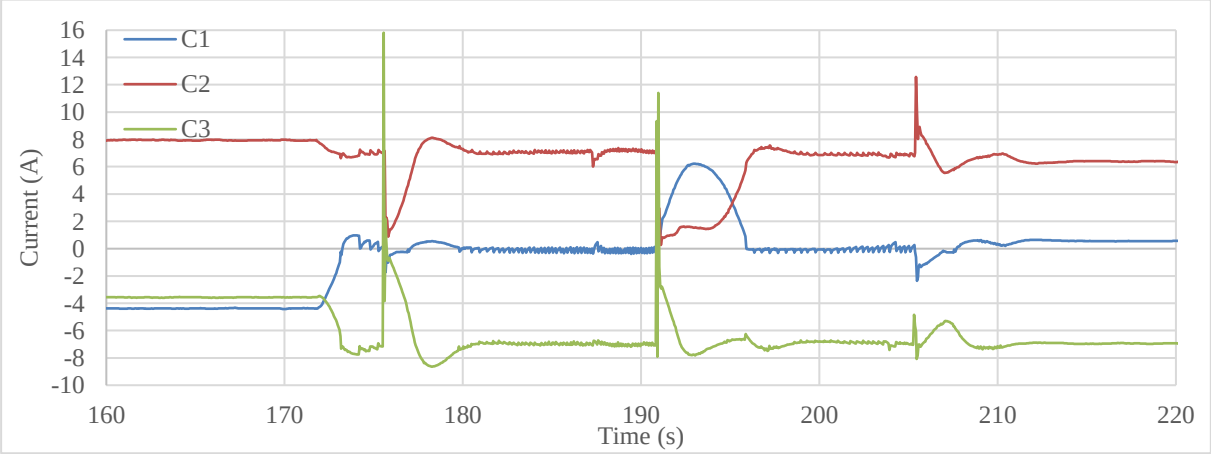

Figure 9: Variation in device output current when the stable voltage is at the nominal 350 V, where the bidirectional controller changes polarity.

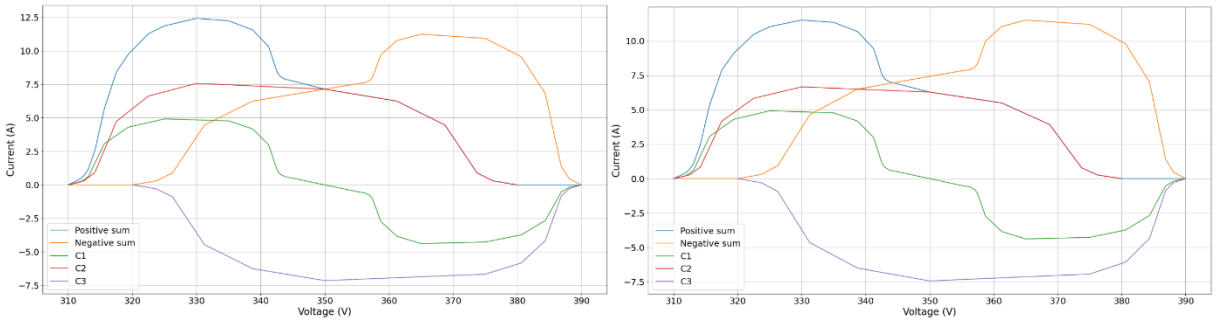

Figure 10: Left) Stable voltage level at nominal 350 V. Right) Reduction in supplied power.

3.2 Stable voltage

The voltage range over which the stable voltage stretches has a large effect on system voltage stability. This is made clear in Fig 11 and Fig 12, in which the stable voltage is reduced from a voltage range to a single point. The situation of a voltage range would happen only in the case that the maximum load power is equal to the maximum source power and exacerbated by having no bidirectional source that would provide a constant change throughout the operational voltage range. A larger overlapping voltage range results in a larger range where the sum of current in the system is 0 A, and thus the voltage wanders. Athough dI/dV at this point is the lowest on the curve, the voltage range is the largest, therefore, with a wide overlap the voltage varied between 350.0 V to 344.5 V as opposed to 351.6 V to 349.2 V with the small overlap. The current variation was comparable for both cases.

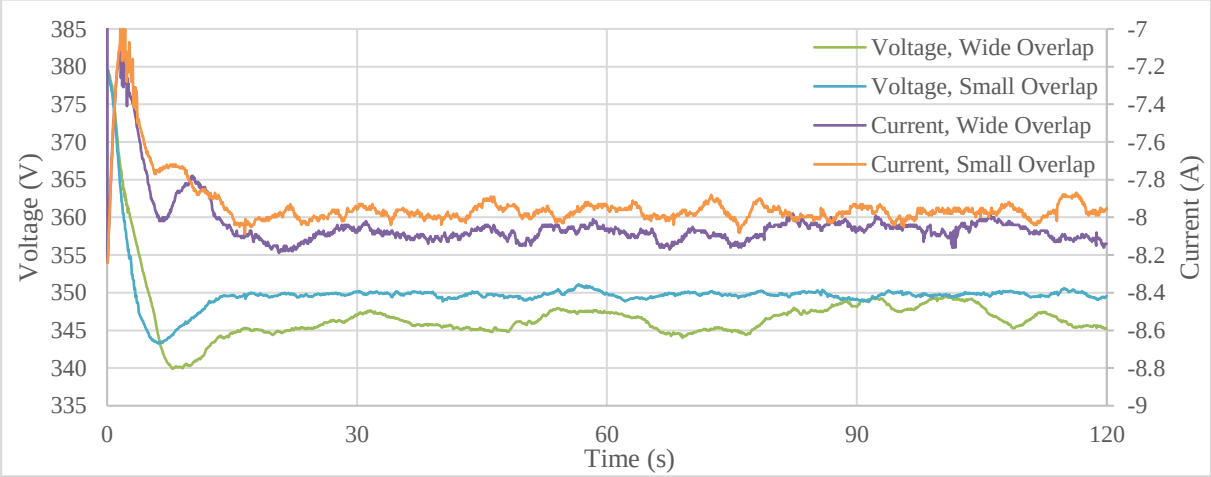

Figure 11: Current and voltage of C3 in the cases of a wide V-I overlap and a narrow V-I overlap.

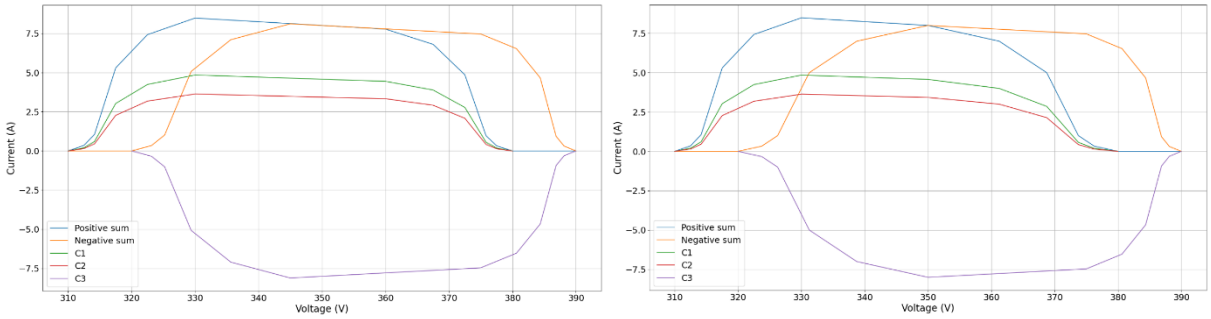

Figure 12: V-I curves of a 2 source, 1 load system. Left) Wide voltage overlap. Right) short voltage overlap

3.3 Effect of N

Without changing any other parameters the number of segments in the piecewise linear droop curve was increased from 3 to 5, at 30 s in Fig 13. Due to the s-shaped curve defined in these tests there would be 5 and 9 segments respectively, since the joining segment is shared by both parts. At this stable voltage the outcome was a steeper curve. More segments meant a smoother and fuller arc to the curve, therefore the first segment would be steeper and the final segment flatter, a higher dI/dV and lower dI/dV, respectively.

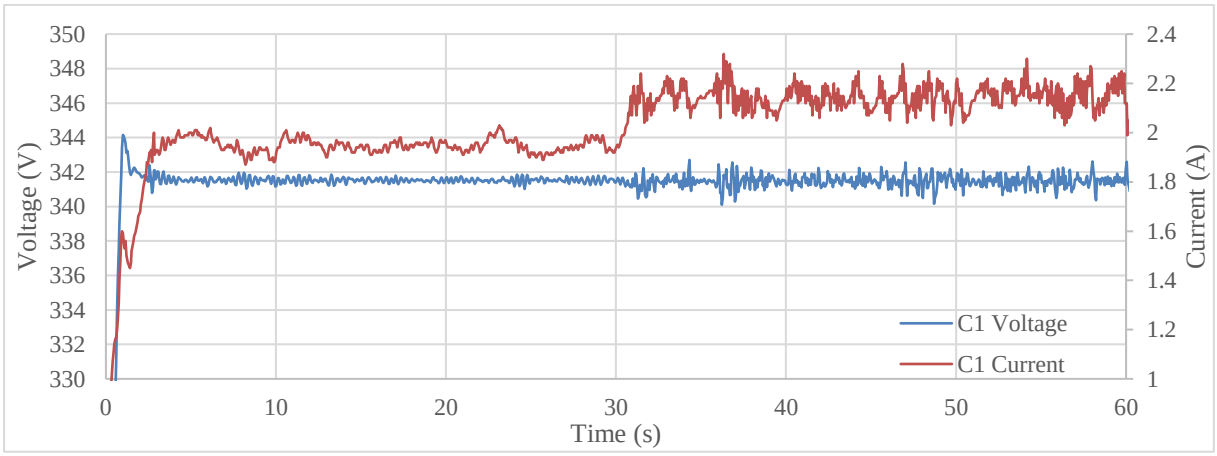

Figure 13: The network voltage stability as measured by C1 and the ouput current of C1 with respect to increasing the number of segments in the PWLD curve, N.

However, as Fig 14 shows the change is visibly negligible. This raises the question, how many segments are optimal? The answer is somewhat convoluted at this stage; it is so dependant on the point in the respective curves the stable voltage occurs. For a given network voltage it may be that for one device a 1 segment linear droop curve is ideal, whilst another may be best suited with 10 segments. Alternatively, the parameters alpha and beta [6] push the curve outwards/inwards. Again, depending on where the stable voltage occurs along the V-I curves, higher values of alpha and beta may make specific segments of the curve shallower or steeper.

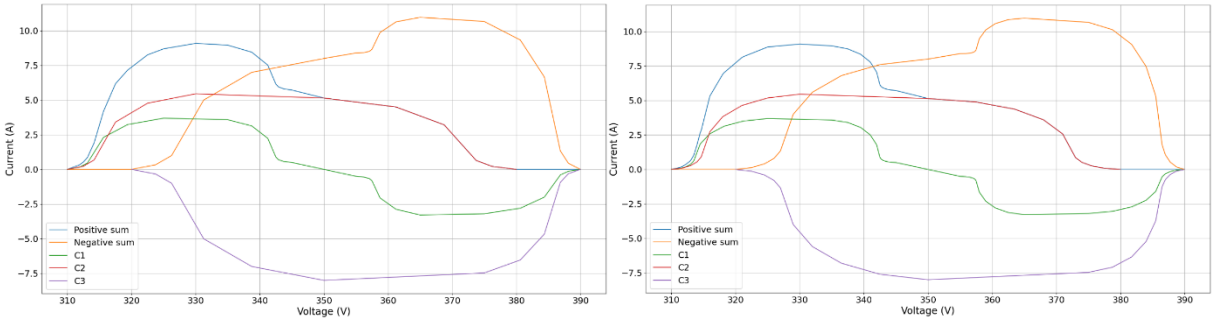

Figure 14: Left) 5 segment PWLD curve. Right) 9 segment PWLD curve.

3.4 Use of 4 devices

The control method was extended to use 4 devices with a similar degree of success, as can be seen in Fig 15 and Fig 16. The system struggled to accurately share the current when the bidirectional device switched polarity but remained at a low output current, due to the rapid switching between source and load or 0 A and a non-zero current. However, when the current of the bidirectional device was constant as either a source or a load, the network voltage remained stable and was influenced only by the aggregated dI/dV of the devices.

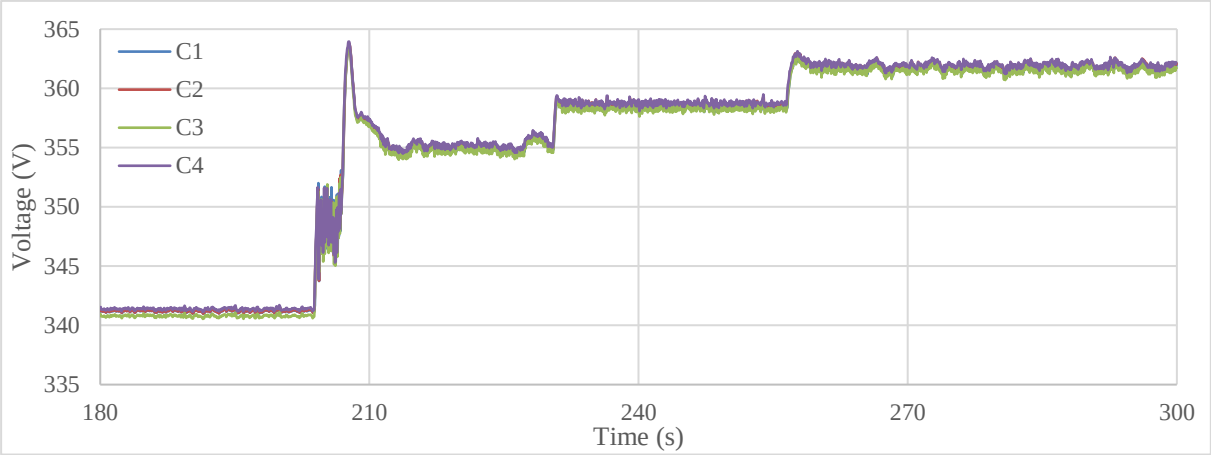

Figure 15: Variation in network voltage due to variations in device output powers

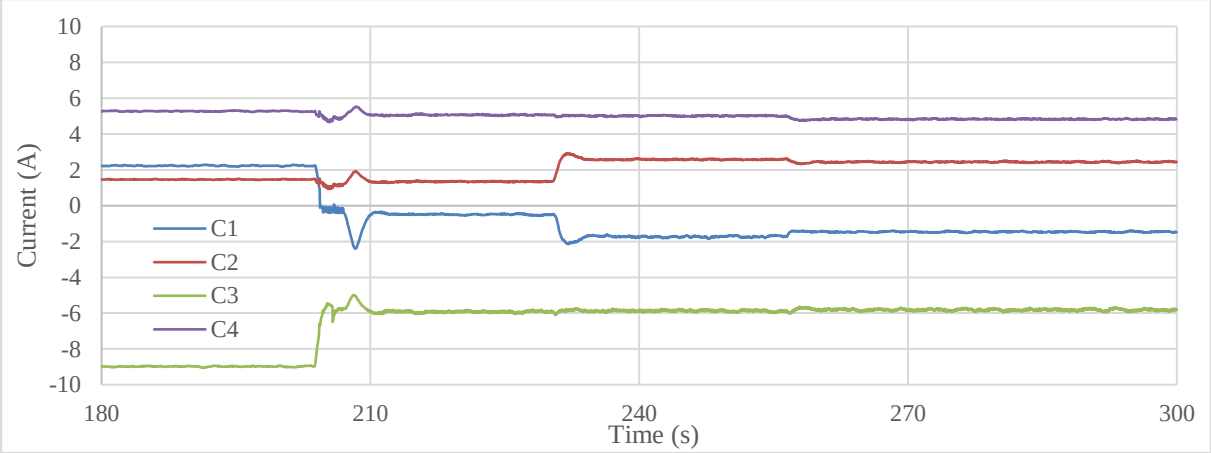

Figure 16: Variation in device output current

4 Discussion and Conclusion

This study has shown the effectiveness of an adapted voltage droop control for multiple devices with varying output powers and polarities, over a wide voltage range. Steady state network voltage stability is achieved for a variety of scenarios, though network voltage stability during dynamic power flow changes sometimes proves challenging. This is the case when a bidirectional device switches polarity causing inaccurate current sharing. The implementation of a deadband around the nominal voltage may improve this response.

The rate of change of current with respect to voltage at the stable voltage level, dI/dV, has a large impact on network voltage stability. If even one device has a high dI/dV the network voltage will see increased instability when compared to the case when all devices have a low dI/dV. This means that careful V-I curve formation is required or that an adaptive dI/dV could be implemented, though no steps have yet been made towards realising this idea.

The piecewise linear droop curve allows for a lower dI/dV across a wider operating bus voltage for pure sources and pure loads. However, at the more extreme voltages, closer to the maximum of 380 V and minimum of 320 V, dI/dV is higher, although those more extreme voltages will be less frequently observed. This is also the difficulty for a bidirectional controller. The PWLD curve introduces two areas of high dI/dV in the middle of the voltage range, and is therefore frequently experienced. It is stipulated that in these regions a linear droop curve or the PWLD curve with alpha and beta coefficients less than 1 could be better suited. The inclusion of the s-shaped piecewise linear droop curve shifts the section of high dI/dV to a voltage level nearer to 350 V, thus increasing the likelihood of operating in that range. Therefore, for devices acting as a pure source or pure load, regular PWLD would be better suited.

There are other factors that may influence the system stability. The control code for the two devices is running simultaneously and in parallel using the Python Multiprocessing library. The time of measurement quickly falls out of synchronisation, thus, one device sets i_{Source} at t_{source} then a fraction of a second later another device sets i_{Load} at t_{Load}, using a different measured voltage. The processing speed of the computer and code results in a slight inconsistency between the instantaneous bus voltage measurement used to determine the new output current and the bus voltage when the new output current is set, approximately 50 ms later. When combined with the previous factor, this could create an oscillatory effect as each device corrects to a slightly different voltage. Additionally, there is a voltage drop due to cable impedance and the load device consistently measures a bus voltage lower than the source device. As such, the stable voltage, as defined in the V-I curves, is never attained exactly by both devices simultaneously. Finally, there is no parallel capacitor connected to absorb/deliver balancing current in response to network voltage changes.

Future work

This project is ongoing and will continue to refine the control code. The implementation of energy flow (kWh) meters and Raspberry PIs for individual device controllers with user interface is expected in the next phase. This should also improve processing time and thus reduce the sample rate.

Acknowledgments

This research is a part of the VAP-DC project funded by RVO. Project number: TGOM120031. I am grateful for the collaboration and data provision from ASR, Venema Technish Bedrijf, Kropman Installatietechniek, and DC Systems.

References

[1] Lu, X., Guerrero, J. M., Sun, K., & Vasquez, J. C. (2013). An improved droop control method for DC microgrids based on low bandwidth communication with DC bus voltage restoration and enhanced current sharing accuracy. *IEEE Transactions on Power Electronics*, *29*(4), 1800-1812.

[2] Dam, D. H., & Lee, H. H. (2018). A power distributed control method for proportional load power sharing and bus voltage restoration in a DC microgrid. *IEEE transactions on industry applications*, *54*(4), 3616-3625.

[3] Guerrero, J. M., Vasquez, J. C., Matas, J., De Vicuña, L. G., & Castilla, M. (2010). Hierarchical control of droop-controlled AC and DC microgrids—A general approach toward standardization. *IEEE Transactions on industrial electronics*, *58*(1), 158-172.

[4] Liu, G., Caldognetto, T., Mattavelli, P., & Magnone, P. (2018). Power-based droop control in dc microgrids enabling seamless disconnection from upstream grids. *IEEE Transactions on Power Electronics*, *34*(3), 2039-2051.

[5] Vu, T. V., Perkins, D., Diaz, F., Gonsoulin, D., Edrington, C. S., & El-Mezyani, T. (2017). Robust adaptive droop control for DC microgrids. *Electric Power Systems Research*, *146*, 95-106.

[6] Hailu, T., & Ferreira, J. A. (2017, December). Piece-wise linear droop control for load sharing in low voltage DC distribution grid. In *2017 IEEE Southern Power Electronics Conference (SPEC)* (pp. 1-6). IEEE.

[7] Neyret, Y. DC Microgrids Principles and Benefits. Technical report, *DC Systems*

[8] Delta Elektronika B.V. (2022, December). SM15K-series Product Manual

[9] Yang, J., Jin, X., Wu, X., Acuna, P., Aguilera, R. P., Morstyn, T., & Agelidis, V. G. (2017). Decentralised control method for DC microgrids with improved current sharing accuracy. *IET Generation, Transmission & Distribution*, *11*(3), 696-706.

Presenter Biography

Edward holds a MSc degree from the Technical University of Delft, the Netherlands, and has been conducting research in the e-mobility sector at the Amsterdam University of Applied Sciences since 2021. His research thus far has included energy modelling and grid integration of electric vehicles.